





[View Journal Online](#)
[View Article Online](#)

Synthesis, physicochemical characterisation and DNA binding study of a novel azo Schiff base Ni(II) complex

Uttam Kumar Singha , Sudarshan Pradhan , Dipu Kumar Mishra , Pritika Gurung , Anmol Chettri , and Biswajit Sinha *

Department of Chemistry, University of North Bengal, Siliguri, 734013, India

* Corresponding author at: Department of Chemistry, University of North Bengal, Siliguri, 734013, India.
 e-mail: biswachem@gmail.com (B. Sinha).

RESEARCH ARTICLE



doi: 10.5155/eurjchem.14.2.280-286.2375

Received: 30 November 2022

Received in revised form: 02 March 2023

Accepted: 11 March 2023

Published online: 30 June 2023

Printed: 30 June 2023

KEYWORDS

CT-DNA

Ni(II) complex

Azo Schiff base

DNA binding study

Molecular docking

DNA cleavage study

ABSTRACT

The azo Schiff base ligand was synthesised, along with its Ni(II) complex, by diazotisation of salicylaldehyde with 4-nitroaniline in accordance with the accepted literature approach. Using a variety of spectroscopic techniques, the resulting complex is analysed both quantitatively and qualitatively (Elemental analysis, FT-IR spectroscopy, UV-VIS spectroscopy, ¹H NMR, etc.). Spectral measurements of the complex revealed a mole ratio of 1:1. The non-electrolytic nature of the complex is confirmed by molar conductance investigation. The unique azo compound had a tetrahedral shape as a result of the tetra coordination of two phenolic oxygen and two imine nitrogen. The ability of the metal complexes to bind DNA was examined using absorption spectroscopy, fluorescence spectroscopy, viscosity tests, and thermal denaturation methods. Experimental research suggests that complexes bind to DNA through intercalation.

Cite this: *Eur. J. Chem.* 2023, 14(2), 280-286

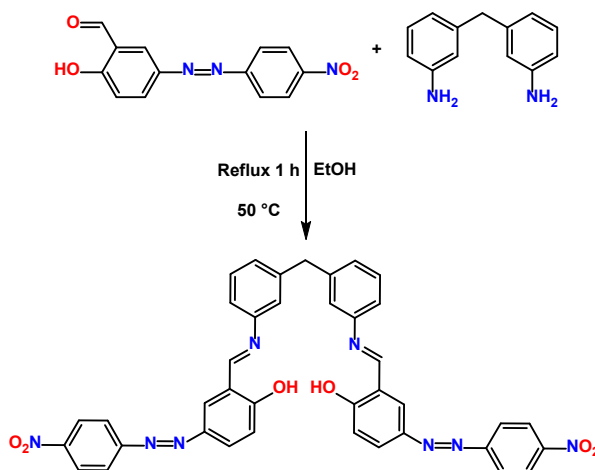
Journal website: www.eurjchem.com

1. Introduction

Azo Schiff bases are compounds having both azo and azomethine groups. The azo group has excellent donor properties which are important in coordination chemistry [1-3]. Azo compounds show biological activities, such as bacterial [4] and pesticidal [5] activities. The azomethine group has good donor properties [6,7] and can form stable complexes with a transition metal ion [8]. Schiff bases are well known to have antifungal [9], antitumor [10], and antibacterial [11-16] activities. Azo Schiff bases are synthesised mostly by coupling a diazonium ion with an aromatic aldehyde to form what is called 'azo aldehyde'. The azo aldehyde is allowed to condense with amines (alkyl or aryl) to form an azo Schiff base. The resulting azo Schiff base possesses azo and azomethine groups in such a way that the coordination of both groups to a metal ion is not affordable. In addition, among the various organic chelating ligands, Schiff bases bearing azo methane linkages are an excellent class of chelating ligands that are able to coordinate various metal ions and stabilise them in various oxidation states and allow the application of Schiff base metal complexes in a variety of catalytic organic transformations [17]. Schiff base metal complexes are also used in many analytical fields, such as

calorimetric sensing of ions, corrosion inhibitors, metal extraction, etc. [18]. During the past decade, considerable attention has been paid to the synthesis and study of azo-azomethane compounds containing hydroxyl groups for intermolecular proton transfer reactions [19]. The thermochromic and/or photochromic behaviour of these classes of compounds can be exploited from the electronic structure of these dyes [20].

In the chemotherapeutic approach to cancer treatment, DNA is the target molecule. The unique properties of the metal atoms present in the drugs help us develop metallopharmaceuticals. *Cis-platin* is an efficient chemotherapeutic agent for treating various types of cancers, such as sarcomas, small cell lung cancer, ovarian cancer, lymphomas, and germ cell tumours. These compounds palatinate the DNA present inside the cell membrane through interstrand and intrastrand cross-linking and the formation of adducts, usually through the amino acid of guanine in the cell, as it is the most electron-rich site and hence easily oxidised. Due to adduct formation, the distortion produced results in the inhibition of DNA replication. In addition to the effectiveness of cisplatin against cancer cells, it has encountered several side effects such as anemia, diarrhea, alopecia, petechia, fatigue, nephrotoxicity, emetogenesis, ototoxicity, and neurotoxicity.



Scheme 1. Synthesis of 2,2'-((1E,1'E)-((methylenebis(3,1-phenylene))bis(azaneylylidene))bis(methaneylylidene))bis(4-((4-nitrophenyl)diazanyl)phenol) (H_2L).

Recently, in the field of radiotherapy or chemotherapy, transition metal complexes are widely used in the treatment of cancer but they follow different mechanisms compared with *cis*-platin and attack the mitochondria. In addition, they enhance DNA damage and make the treatment target selective. However, azo-azomethane-based transition-metal complexes are very rare.

Nickel is a micronutrient essential for the proper functioning of the human body, as it increases hormonal activity and is involved in lipid metabolism. This metal makes its way to the human body through the respiratory tract, digestive system, and skin. When nickel enters the body, it is distributed to all organs, but mainly in the kidney, bone, and lungs. Nickel is found in the body at the highest concentrations in nucleic acids, DNA, and RNA, and is thought to be somehow involved in protein structure or function. It may activate certain enzymes related to glucose breakdown or utilisation. Nickel may aid in prolactin production and thus be involved in human breast milk production. Nickel aids in iron absorption, as well as adrenaline and glucose metabolism, hormones, lipids, cell membrane, improves bone strength and may also play a role in the production of red blood cells. The DNA interaction study of the nickel-based metal complex is still to be explored. So, in this research, we have reported the synthesis and physicochemical characterisation of a new Ni(II) complex and studied its DNA interaction ability.

2. Experimental

2.1. Materials and methods

3,3'-Methylenedianiline, salicylaldehyde, 4-nitroaniline, nickel(II) acetate, CT-DNA and ethidium bromide (EB) were purchased from Sigma-Aldrich. Solvents (including absolute ethyl alcohol, diethyl ether, dimethyl sulfoxide, etc.) were purchased from SD Fine Chemicals, India. Solvents were purified prior to use following a standard procedure from the literature.

2.2. Physical measurements

The percentage composition of C, H, and N of the complex and ligand was determined using the micro analytical method on a Perkin Elmer 240C elemental analyser (USA). FT-IR spectra of the ligand and its complex were recorded by using KBr pellets in the 4000-400 cm^{-1} range using an FT-IR spectrophotometer. The UV-visible spectra of the ligand and its metal complexes were carried out in DMSO using a Jasco V-530

UV-vis spectrophotometer. NMR spectra were recorded on a Bruker 400 MHz FT-NMR instrument using $\text{DMSO-}d_6$ as solvent and tetramethylsilane $[\text{Si}(\text{CH}_3)_4]$ as an internal standard. The melting point of the ligand and the decomposition temperature of the complex were determined using the open capillary method. A fluorescence emission experiment was carried out on a JASCO V-530 Spectrophotometer at room temperature.

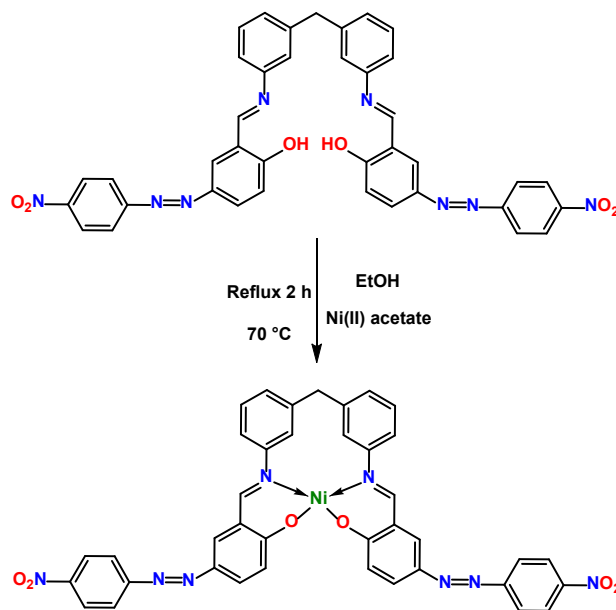
2.3. Synthesis of 2-hydroxy-5-(4-nitrophenylazo)benzaldehyde

The azo derivative of salicylaldehyde was prepared by diazotisation of salicylaldehyde with 4-nitroaniline following the standard literature procedure. In a typical experiment, salicylaldehyde (1.22 g, 10 mmol) was dissolved in water (15 mL) containing 0.4 g (10 mmol) of NaOH and 4.24 g (40 mmol) of Na_2CO_3 for 30 minutes at 0 °C in 50 mL beaker. In another beaker, 4-nitroaniline (10 mmol) was dissolved in water by adding concentrated HCl in a required amount. The solution was then cooled in a nice bath at 0 °C and solid NaNO_2 (10 mmol) was added slowly to the solution with constant stirring. The salicylaldehyde solution was added dropwise to the resulting diazonium chloride solution with constant stirring and the temperature was maintained at 0 °C during the coupling time. At 0 °C, the reaction mixture was stirred for an hour before gently heating to room temperature. Filtering was used to collect the reddish product, which was then rinsed with 100 mL of 10% NaCl solution (Scheme 1).

2.4. Synthesis of ligand, H_2L

An ethanolic solution of 2-hydroxy-5-(4-nitrophenylazo)benzaldehyde (0.2 mol) was dropwise added to a hot ethanolic solution of 3,3'-methylenedianiline (0.1 mol) and refluxed for 1 hour. The resulting brick-red coloured ligand was filtered numerous times, washed with ethanol, and ether, and then vacuum desiccated to dry it. The synthesis of the ligand (H_2L) is shown in Scheme 1.

2,2'-((1E,1'E)-((methylenebis(3,1-phenylene))bis(azaneylylidene))bis(methaneylylidene))bis(4-((4-nitrophenyl)diazanyl)phenol) (H_2L): Color: Brick red. Yield: 82%. M.p.: >250 °C. FT-IR (KBr, ν , cm^{-1}): 3447 (OH), 1618 (C=N), 1099 (C-O). ^1H NMR (400 MHz, $\text{DMSO-}d_6$, δ , ppm): 9.88 (s, 2H, OH), 9.29 (s, 2H, -CH=N-), 8.45-6.55 (m, 22H, Ar-H), 3.75 (s, 2H, CH_2). Anal. calcd. for $\text{C}_{39}\text{H}_{28}\text{N}_8\text{O}_6$: C, 66.47; H, 4.01; N, 15.90. Found: C, 66.65; H, 3.93; N, 15.95%. UV/Vis (DMSO , λ_{max} , nm): 430 ($n\text{-}\pi^*$), 372 ($\pi\text{-}\pi^*$).



Scheme 2. Synthesis of Ni(II) complex.

2.5. Synthesis of Ni(II) complex

By mixing an equimolar amount of an ethanolic solution of the synthesised ligand H_2L with an ethanolic solution of Ni(II) acetate, the metal complex was synthesised. The resulting reaction mixture was then refluxed for two hours at 70 °C, during which time the Ni(II) metal complex precipitated. The brown precipitate was removed by filtering, washing with ethanol and drying in a vacuum desiccator (Scheme 2). Color: Brown. Yield: 79%. M.p.: >250 °C. FT-IR (KBr, ν , cm^{-1}): 1599 (C=N), 1065 (C-O), 580 (Ni-O), 488 (Ni-N). 1H NMR (400 MHz, DMSO- d_6 , δ , ppm): 8.57 (s, 2H, -CH=N-), 6.91-8.75 (m, 22H, Ar-H), 3.60 (s, 2H, CH₂). Anal. calcd. for C₃₉H₂₆N₈O₆Ni: C, 61.52; H, 3.44; N, 14.72. Found: C, 61.98; H, 3.32; N, 14.77%. UV/Vis (DMSO, λ_{max} , nm): 360 (π - π^*), 325 (d - d), 275 (π - π^*).

3. Results and discussion

3.1. Characterization of the ligand and its Ni(II) complex

According to elemental and other spectroscopic analyses, all of the synthesised compounds, which are air stable, were successfully prepared and both the ligand and the metal complex are DMSO soluble and moisture insensitive. The analytical data agree well with the calculated values and support the formation of mononuclear Ni(II) complexes with metal-to-ligand ratio of 1: 1. The measured molar conductance of the complex in DMSO for a $\sim 1 \times 10^{-3}$ M at ambient temperature is 13 which is consistent with the fact that the complex is not electrolytic in nature [21].

To obtain a conclusive idea about the mode of coordination of the ligand with the metal ion and the structure of the metal complex, we compared the main IR bands of the metal complex with those of the ligand. The appearance of a strong band at 1450 cm^{-1} in the IR spectra of 2-hydroxy-5-(4-nitrophenylazo) benzaldehyde confirms the diazotisation. The FT-IR spectra of the ligand (H_2L) showed a strong broad absorption band at 3447 cm^{-1} ; This band was assigned to the OH of the ligand. This OH band vanished in the Ni(II) complex, indicating the involvement of the oxygen atom of the OH group in the coordination of the Ni(II) ion. Azomethine $\nu(C=N)$ causes the Schiff base to exhibit a recognisable strong band at 1618 cm^{-1} . This band shifts to 1599 cm^{-1} in the complex, demonstrating the

involvement of azo methane nitrogen in complexation [21]. The shift in the $\nu(C-O)$ band of the ligand from a higher frequency at 1099 cm^{-1} to a lower frequency at 1065 cm^{-1} in the Ni(II) complex provides additional evidence that the O atom of the phenolic OH group coordinates with a metal ion. The formation of two non-ligand bands at 580 and 488 cm^{-1} attributable to (Ni-O) and (Ni-N), respectively, in the FT-IR spectra of the complex confirms the involvement of phenolic O and azomethine N in the complexation. As a result, the FT-IR results point to the possibility of a tetrahedral geometry for the Schiff base ligand, which is coupled to Ni(II) via azomethine N and deprotonated phenolic O.

The presence of azomethine proton (-CH=N-) caused the synthesised Schiff base to exhibit a singlet at about δ 9.29 ppm [22]. However, in the presence of the complex, this -CH=N- peak is displaced to δ 8.57 ppm, indicating that azomethine nitrogen was involved in the coordination of Ni(II). Furthermore, the ligand displayed a signal at δ 9.88 ppm due to a proton of the hydroxyl group (OH), which vanishes in the compound and indicates that the OH group was deprotonated during complexation [23]. All azo-azomethine compounds showed multiplet aromatic protons in the range of δ 6.91-8.45 ppm.

The synthesised azo-azo methane derivative (H_2L) and its metal complex's the UV-Visible spectra were recorded in DMSO at ambient temperature. The electronic absorption spectra of the ligand (H_2L) showed mainly two types of bands. The first band at 372 nm can be attributed to the π - π^* energy changes of the aromatic ring, while the $n \rightarrow \pi^*$ transition of the azo and azo methane chromophore causes the second band at 430 nm. During complexation, the $\pi \rightarrow \pi^*$ band and the $n \rightarrow \pi^*$ bands experience a blue shift. Furthermore, there is a hump that appeared near 325 nm and is related to the $d \rightarrow d$ transition [23].

3.2. DNA binding study

3.2.1. Electronic absorption titration

A key approach to examine how DNA interacts with small compounds is to study the interaction through absorption spectroscopic titration. Changes in absorbance and wavelength arise from the binding of a metal complex to DNA in an intercalative manner.

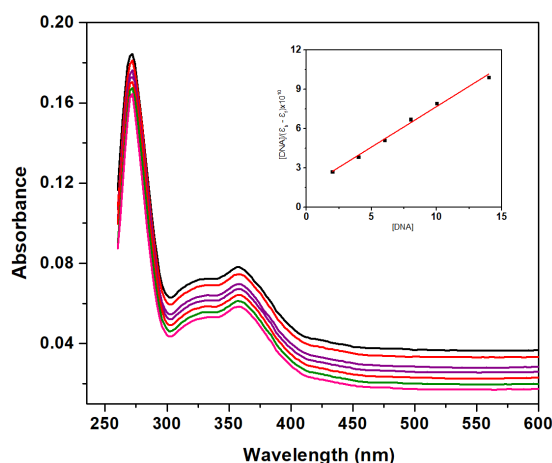


Figure 1. Absorption spectra of the Ni(II) complex in the absence and presence of CT-DNA at increasing concentrations (0-15 μM), Inset: plot for the binding constant (K_b).

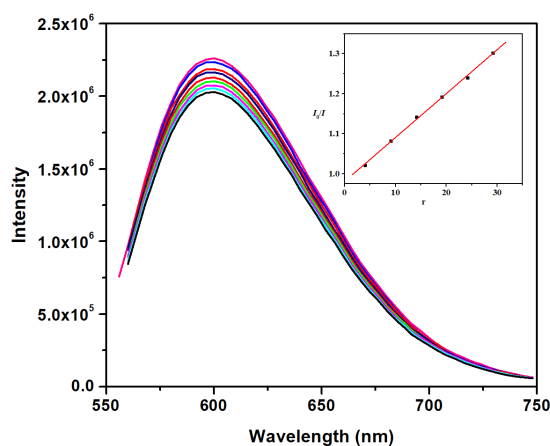


Figure 2. DNA-bound EB emission spectra in the absence and presence of an increasingly Ni(II) complex (0-30 μM), Inset: plot for the quenching constant (K_{sv}).

In a solvent mixture of 1% DMSO and 99% Tris-HCl buffer, the binding affinity of the metal complex with CT-DNA was investigated using a fixed concentration of the complex to which increasing amounts of CT-DNA solution were added. To eliminate the absorbance of free CT-DNA, an equal amount of CT-DNA was added to the complex solution chamber and the reference chamber before recording the absorption spectra. Strong stacking interactions between DNA base pairs and aromatic chromophores, which point to an intercalating mechanism of binding, caused changes in absorbance and wavelength (2.5 nm for the $n \rightarrow \pi^*$ band) as DNA was added to the chamber of complex solution in stages (Figure 1) [24]. Utilising the Wolfe-Shimer equation, the intrinsic binding constant (K_b) was calculated to calculate the capacity of the metal complex to bind to CT-DNA:

$$[\text{DNA}]/(\epsilon_a - \epsilon_f) = [\text{DNA}]/(\epsilon_b - \epsilon_f) + 1/K_b(\epsilon_a - \epsilon_f) \quad (1)$$

and the value of K_b is $(2.1 \pm 0.2) \times 10^4 \text{ M}^{-1}$.

3.2.2. Fluorescence emission spectroscopy

An ethidium bromide (EB) displacement technique was used in a competitive binding experiment to confirm the manner of binding of the complex to CT-DNA. Due to the planar phenanthridine ring of EB intercalating between adjacent DNA base pairs, the EB-DNA couple exhibits a strong emission band at 592 nm [25]. If a foreign molecule that can intercalate to DNA

equally or more strongly than EB is added to the EB-DNA solution, the emission band of the EB-DNA couple will be noticeably quenched [26]. In tris-HCl buffer, the competitive binding experiment was carried out while maintaining $[\text{DNA}]/[\text{EB}] = 1.13$ and increasing the concentration of the complex. The intensity of the emission in the EB-DNA solution decreased significantly with the addition of Ni(II) complex solution (Figure 2). This decrease in the EB-DNA emission intensity after the addition of the Ni(II) complex points to the EB displacement, which can be distinguished as an intercalative manner of binding. Using the conventional Stern-Volmer equation, the quenching constant or quenching strength (K_{sv}) of the complex toward the EB-DNA conjugate was further calculated. $I_0/I = 1 + K_{sv} \times r$, where I and I_0 are the fluorescence intensities in the presence and absence of the quencher and r is the ratio of the total concentration of the complex to that of DNA. The calculated value of K_{sv} for the Ni(II) complex is $(1.8 \pm 0.3) \times 10^4 \text{ M}^{-1}$. Therefore, the observed quenching suggests the remarkable ability of the Ni(II) complex to displace the intercalator EB from the EB-DNA conjugate and indirectly reveal the intercalative mode of binding to DNA.

3.2.3. DNA melting study

The study of DNA melting is a crucial tool for determining the degree of intercalation. The melting temperature increases as a result of the intercalation of foreign molecules into DNA base pairs (T_m).

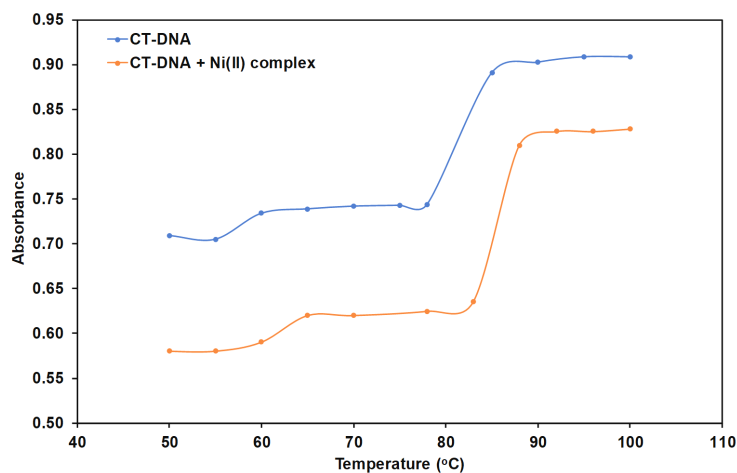


Figure 3. Plot of absorbance versus temperature (°C) for the melting of CT-DNA alone and the CT-DNA + Ni(II) complex.

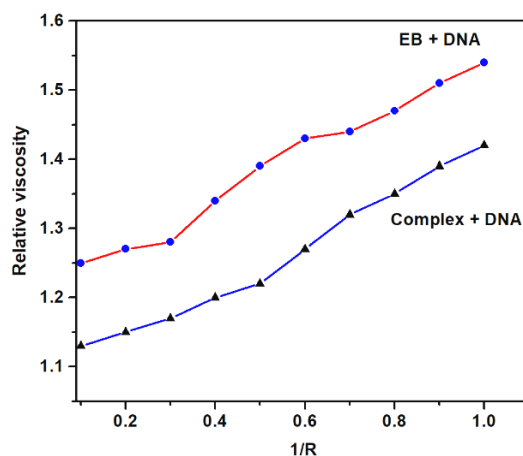


Figure 4. Effect of increasing amounts of EB and Ni(II) complex on the relative viscosity of CT-DNA.

To conduct this experiment, solutions of CT-DNA and the complex were made in a solvent mixture of 1% DMSO and 99% Tris-HCl buffer. The melting curve of the CT-DNA solution is shown in Figure 3 in both the absence and the presence of the Ni(II) complex. When the Ni(II) complex was included, the measured T_m for the CT-DNA solution increased substantially to 88.0 °C. Increased T_m value encourages intercalative binding of the Ni(II) complex [27].

3.2.4. Viscosity measurement

Hydrodynamic tactics (like viscosity measurement), which are sensitive to the length of DNA, are substantial tools for investigating the binding mode of metal complexes to DNA. An intercalative mode of interaction results in an increase in viscosity values because of the lengthening of the DNA helix. Viscosity measurements were carried out using a capillary viscometer (Ostwald viscometer) thermostated at 25 ± 1 °C keeping the concentration of CT-DNA (100 μ M) constant while varying the concentration of the complex (10-100 μ M). The relative viscosity of DNA in the absence (η_0) and presence (η) of the Ni (II) complex was measured using the relation: $\eta = (t - t_0)/t_0$, where t is the flow time of the CT-DNA complex solution and t_0 is the flow time of the buffer alone in seconds. The results obtained were represented as $(\eta/\eta_0)^{1/3}$ versus $1/R$ ($R = [\text{DNA}]/[\text{Complex}]$). Here, with increasing concentration of the Ni(II) complex, the relative viscosity of DNA increases sharply, similar to the nature of the well-known intercalator EB (Figure 4) suggesting intercalative binding.

3.2.5. DNA cleavage study

pUC19 DNA solutions were prepared and diluted with loading dye using 1% agarose gel to perform cleavage assays. 3 μ L of EB (0.5 μ g/mL) was added to each solution and thoroughly mixed. The following stage involved the pouring of warm agarose and immediately using a comb to hold it securely to form sample wells. A sufficient amount of electrophoretic buffers was added to the gel in the electrophoretic tank to completely encapsulate it at a depth of 1 mm. The loading dye was combined with the DNA sample (20 μ M), 30 μ M complex, and 10 μ M H_2O_2 in the aforementioned buffer (pH = 7.2) and then pipetted into the well of the submerged gel. A 50 mA electric current was passed and the gel was taken out from the buffer. After the gel had undergone electrophoresis using various concentrations of Ni(II) complex in the presence of H_2O_2 , it was photographed under UV light. DNA is converted from its supercoiled (Form I), nicked (Form II), and linear (Form III), determining the capacity of the complex to cleave DNA (Form III) [28]. The result of DNA cleavage is shown in Figure 5.

Control experiments (lanes 1 and 2) and in the presence of ligand (lane 3) show no DNA cleavage because there is no metal complex in role; however, increasing the concentration of the complex (lanes 4-6) shows that the percentage of Form I steadily decreases while Form II increases. This suggests that the complex acted on supercoiled plasmid DNA, as there was a significant difference in the complex bands compared to the control DNA bands. However, there is no discernible difference

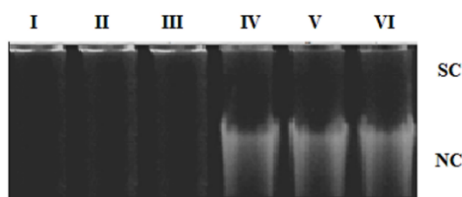


Figure 5. Changes in the electrophoretic pattern of the agarose gel of the plasmid DNA of pBR322 induced by H_2O_2 for the ligand and Ni(II) complex. Lane (I): DNA control, Lane (II): DNA + H_2O_2 , Lane (III): DNA+ 10 μ M ligand + H_2O_2 , Lane (IV-VI): DNA + Ni(II) complex + H_2O_2 , [complex] = 5, 10, 15 μ M, respectively.

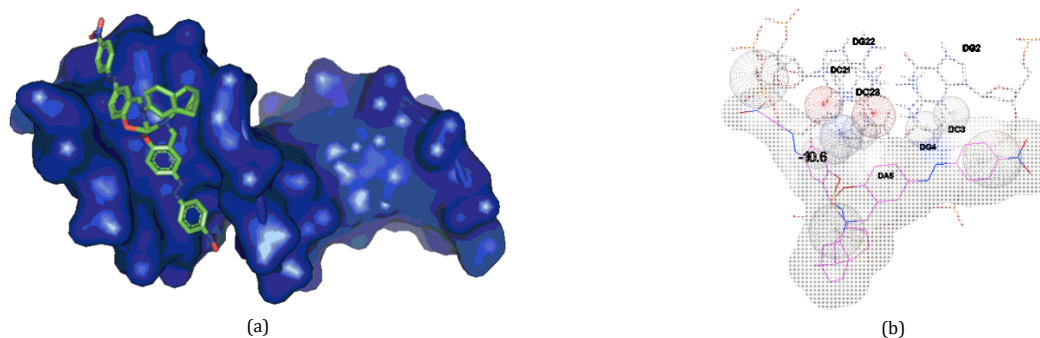


Figure 6. (a) Molecular surface view of the protein molecule and the complex molecule docked at its binding site. (b) The molecular interaction of the DNA dodecamer with the synthesised complex.

in the bands between ligand and control DNA. The experiment is influenced by hydroxyl radicals or peroxy species released by H_2O_2 . The presence of smears in the gel photograph suggests radical cleavage [29]. Various research groups have reported the detailed mechanism of DNA cleavage by a metal complex in the presence of H_2O_2 [30]. Because the synthesised complex is efficient in cleaving the supercoiled plasmid DNA into an open circular form, it can be inferred that the complex may inhibit pathogen growth by cleaving the genome.

3.3. Molecular modeling analysis

The AutoDock Vina programme was used to perform molecular docking experiments (version 1.1.2). The RCSB PDB (<https://www.rcsb.org>) was used to extract the X-ray crystallographic structure of the receptor protein, which was then used for molecular docking studies against the Ni(II) complex. The PDB ID for the protein with receptor structure is 1BNA, and the grid dimensions for the x , y , and z axes range from 44, 50, and 80. By eliminating the water molecules and adding polar hydrogens, the protein of interest was prepared. The Ni(II) complex displayed distinctive DNA binding and cleaving capabilities, according to the study of DNA interactions. These earlier assertions are therefore supported by a high affinity of magnitude -10.6 kcal/mol in the auto-dock Vina environment. Overall, the results show that the Ni(II) complex interacts strongly with DNA (Figure 6).

4. Conclusions

In this paper, a novel azo-azomethane Schiff base and its Ni(II) complex have been synthesised and characterised by using different physical and spectroscopic techniques. All analytical results suggest the tetrahedral geometry of the synthesised complex. The DNA binding to the Ni(II) complex was studied using CT-DNA and it indicates that the synthesised complex can act as a metallo intercalator. Furthermore, the molecular docking of the Ni(II) complex was carried out using Autodock vina tools. A receptor protein 1BNA was used for docking and a high affinity of magnitude -10.6 kcal/mol was obtained which gave depth to the earlier findings.

Acknowledgements

The authors would like to acknowledge the Departmental Special Assistance Scheme under the University Grants Commission, New Delhi (SAP-DRS-III, No.540/12/DRS/2013) and the University of North Bengal, Government of West Bengal for financial and instrumental support. The authors also acknowledge "Council of Scientific and Industrial Research-Central Salt and Marine Chemicals Research Institute (CSIR-CSMCRI) Bhavnagar, Gujarat, India for elemental analysis.

Disclosure statement

Conflict of interest: The authors declare that they have no conflict of interest. Ethical approval: All ethical guidelines have been adhered to. Sample availability: Samples of the compounds are available from the author.

CRedit authorship contribution statement

Conceptualization: Dipu Kumar Mishra; Methodology: Uttam Kumar Singha; Software: Sudarshan Pradhan; Formal Analysis: Pritika Gurung, Anmol Chettri; Writing - Original Draft: Uttam Kumar Singha; Writing - Review and Editing: Biswajit Sinha.

ORCID iD and Email

Uttam Kumar Singha
 ✉ ukrs1991@gmail.com
 iD <https://orcid.org/0000-0003-4460-0676>
 Sudarshan Pradhan
 ✉ sudarshanpradhan43@gmail.com
 iD <https://orcid.org/0000-0002-6963-8980>
 Dipu Kumar Mishra
 ✉ dipukumarmishra@gmail.com
 iD <https://orcid.org/0000-0002-0743-5627>
 Pritika Gurung
 ✉ pritikagurung21@gmail.com
 iD <https://orcid.org/0000-0003-2074-0711>
 Anmol Chettri
 ✉ chettrianmol5@gmail.com
 iD <https://orcid.org/0000-0002-7939-238X>
 Biswajit Sinha
 ✉ biswachem@gmail.com
 iD <https://orcid.org/0000-0003-0468-4035>

References

- [1]. More, M. S.; Joshi, P. G.; Mishra, Y. K.; Khanna, P. K. Metal complexes driven from Schiff bases and semicarbazones for biomedical and allied applications: a review. *Mater. Today Chem.* **2019**, *14*, 100195.
- [2]. Zhao, P.; Zhai, S.; Dong, J.; Gao, L.; Liu, X.; Wang, L.; Kong, J.; Li, L. Synthesis, structure, DNA interaction, and SOD activity of three nickel(II) complexes containing L-phenylalanine Schiff base and 1,10-phenanthroline. *Bioinorg. Chem. Appl.* **2018**, *2018*, 1–16.
- [3]. Andruh, M. The exceptionally rich coordination chemistry generated by Schiff-base ligands derived from o-vanillin. *Dalton Trans.* **2015**, *44*, 16633–16653.
- [4]. Charo, J.; Lindencrona, J. A.; Carlson, L.-M.; Hinkula, J.; Kiessling, R. Protective efficacy of a DNA influenza virus vaccine is markedly increased by the coadministration of a Schiff base-forming drug. *J. Virol.* **2004**, *78*, 11321–11326.
- [5]. Arunadevi, A.; Raman, N. Biological response of Schiff base metal complexes incorporating amino acids – a short review. *J. Coord. Chem.* **2020**, *73*, 2095–2116.
- [6]. Ommenya, F. K.; Nyawade, E. A.; Andala, D. M.; Kinyua, J. Synthesis, characterization and antibacterial activity of Schiff base, 4-chloro-2-(E)-[(4-fluorophenyl)imino]methylphenol metal (II) complexes. *J. Chem.* **2020**, *2020*, 1–8.
- [7]. de Fátima, A.; Pereira, C. de P.; Olímpio, C. R. S. D. G.; de Freitas Oliveira, B. G.; Franco, L. L.; da Silva, P. H. C. Schiff bases and their metal complexes as urease inhibitors – A brief review. *J. Adv. Res.* **2018**, *13*, 113–126.
- [8]. Wesley Jeevadason, A.; Kalidasa Murugavel, K.; Neelakantan, M. A. Review on Schiff bases and their metal complexes as organic photovoltaic materials. *Renew. Sustain. Energy Rev.* **2014**, *36*, 220–227.
- [9]. Hannon, M. J. Metal-based anticancer drugs: From a past anchored in platinum chemistry to a post-genomic future of diverse chemistry and biology. *Pure Appl. Chem.* **2007**, *79*, 2243–2261.
- [10]. Maksimoska, J.; Feng, L.; Harms, K.; Yi, C.; Kissil, J.; Marmorstein, R.; Meggers, E. Targeting large kinase active site with rigid, bulky octahedral ruthenium complexes. *J. Am. Chem. Soc.* **2008**, *130*, 15764–15765.
- [11]. Catalano, A.; Sinicropi, M. S.; Iacopetta, D.; Ceramella, J.; Mariconda, A.; Rosano, C.; Scali, E.; Saturnino, C.; Longo, P. A review on the advancements in the field of metal complexes with Schiff bases as antiproliferative agents. *Appl. Sci. (Basel)* **2021**, *11*, 6027.
- [12]. Junicke, H.; Hart, J. R.; Kisko, J.; Glebov, O.; Kirsch, I. R.; Barton, J. K. A rhodium(III) complex for high-affinity DNA base-pair mismatch recognition. *Proc. Natl. Acad. Sci. U. S. A.* **2003**, *100*, 3737–3742.
- [13]. Al Zoubi, W.; Al-Hamdani, A. A. S.; Ahmed, S. D.; Ko, Y. G. Synthesis, characterization, and biological activity of Schiff bases metal complexes. *J. Phys. Org. Chem.* **2018**, *31*, e3752.
- [14]. El-Sonbati, A. Z.; Mahmoud, W. H.; Mohamed, G. G.; Diab, M. A.; Morgan, S. M.; Abbas, S. Y. Synthesis, characterization of Schiff base metal complexes and their biological investigation: Synthesis, characterization of Schiff base metal complexes. *Appl. Organomet. Chem.* **2019**, e5048.
- [15]. Mal, S. K.; Chattopadhyay, T.; Fathima, A.; Purohit, C. S.; Kiran, M. S.; Nair, B. U.; Ghosh, R. Synthesis and structural characterization of a vanadium(V)-pyridylbenzimidazole complex: DNA binding and anticancer activity. *Polyhedron* **2017**, *126*, 23–27.
- [16]. Naureen, B.; Miana, G. A.; Shahid, K.; Asghar, M.; Tanveer, S.; Sarwar, A. Iron (III) and zinc (II) monodentate Schiff base metal complexes: Synthesis, characterisation and biological activities. *J. Mol. Struct.* **2021**, *1231*, 129946.
- [17]. Osypiuk, D.; Cristóvão, B.; Bartyzel, A. New coordination compounds of CuII with Schiff base ligands—crystal structure, thermal, and spectral investigations. *Crystals (Basel)* **2020**, *10*, 1004.
- [18]. Malinowski, J.; Zych, D.; Jacewicz, D.; Gawdzik, B.; Drzeżdżon, J. Application of coordination compounds with transition metal ions in the chemical industry-A review. *Int. J. Mol. Sci.* **2020**, *21*, 5443.
- [19]. Barton, J. K.; Olmon, E. D.; Sontz, P. A. Metal complexes for DNA-mediated charge transport. *Coord. Chem. Rev.* **2011**, *255*, 619–634.
- [20]. Sahu, G.; Tiekink, E. R. T.; Dinda, R. Study of DNA interaction and cytotoxicity activity of oxidovanadium(V) complexes with ONO donor Schiff base ligands. *Inorganics* **2021**, *9*, 66.
- [21]. Palanimurugan, A.; Dhanalakshmi, A.; Selvapandian, P.; Kulandaisamy, A. Electrochemical behavior, structural, morphological, Calf Thymus-DNA interaction and in-vitro antimicrobial studies of synthesized Schiff base transition metal complexes. *Heliyon* **2019**, *5*, e02039.
- [22]. Khalil, M. M. H.; Ismail, E. H.; Mohamed, G. G.; Zayed, E. M.; Badr, A. Synthesis and characterization of a novel schiff base metal complexes and their application in determination of iron in different types of natural water. *Open J. Inorg. Chem.* **2012**, *02*, 13–21.
- [23]. Tan, C.; Liu, J.; Chen, L.; Shi, S.; Ji, L. Synthesis, structural characteristics, DNA binding properties and cytotoxicity studies of a series of Ru(III) complexes. *J. Inorg. Biochem.* **2008**, *102*, 1644–1653.
- [24]. Haghghi, F. H.; Hadadzadeh, H.; Darabi, F.; Jannesari, Z.; Ebrahimi, M.; Khayamian, T.; Salimi, M.; Rudbari, H. A. Polypyridyl Ni(II) complex, [Ni(tppz)₂]²⁺: Structure, DNA- and BSA binding and molecular modeling. *Polyhedron* **2013**, *65*, 16–30.
- [25]. Gurusamy, S.; Krishnaveni, K.; Sankarganesh, M.; Nandini Asha, R.; Mathavan, A. Synthesis, characterization, DNA interaction, BSA/HSA binding activities of VO(IV), Cu(II) and Zn(II) Schiff base complexes and its molecular docking with biomolecules. *J. Mol. Liq.* **2022**, *345*, 117045.
- [26]. Packianathan, S.; Kumaravel, G.; Raman, N. DNA interaction, antimicrobial and molecular docking studies of biologically interesting Schiff base complexes incorporating 4-formyl-N,N -dimethylaniline and propylenediamine: DNA interaction, antimicrobial and molecular docking studies. *Appl. Organomet. Chem.* **2017**, *31*, e3577.
- [27]. Bheemarasetti, M.; Palakuri, K.; Raj, S.; Saudagar, P.; Gandamalla, D.; Yellu, N. R.; Kotha, L. R. Novel Schiff base metal complexes: synthesis, characterization, DNA binding, DNA cleavage and molecular docking studies. *J. Iran. Chem. Soc.* **2018**, *15*, 1377–1389.
- [28]. Rambabu, A.; Pradeep Kumar, M.; Tejaswi, S.; Vamsikrishna, N.; Shivaraj DNA interaction, antimicrobial studies of newly synthesized copper (II) complexes with 2-amino-6-(trifluoromethoxy)benzo thiazole Schiff base ligands. *J. Photochem. Photobiol. B* **2016**, *165*, 147–156.
- [29]. Rao, N. N.; Kishan, E.; Gopichand, K.; Nagaraju, R.; Ganai, A. M.; Rao, P. V. Design, synthesis, spectral characterization, DNA binding, photo cleavage and antibacterial studies of transition metal complexes of benzothiazole Schiff base. *Chem. Data Coll.* **2020**, *27*, 100368.
- [30]. Mishra, D. K.; Singha, U. K.; Das, A.; Dutta, S.; Kar, P.; Chakraborty, A.; Sen, A.; Sinha, B. DNA Binding, amelioration of oxidative stress, and molecular docking study of Zn(II) metal complex of a new Schiff base ligand. *J. Coord. Chem.* **2018**, *71*, 2165–2182.



Copyright © 2023 by Authors. This work is published and licensed by Atlanta Publishing House LLC, Atlanta, GA, USA. The full terms of this license are available at <http://www.eurjchem.com/index.php/eurjchem/pages/view/terms> and incorporate the Creative Commons Attribution-Non Commercial (CC BY NC) (International, v4.0) License (<http://creativecommons.org/licenses/by-nc/4.0>). By accessing the work, you hereby accept the Terms. This is an open access article distributed under the terms and conditions of the CC BY NC License, which permits unrestricted non-commercial use, distribution, and reproduction in any medium, provided the original work is properly cited without any further permission from Atlanta Publishing House LLC (European Journal of Chemistry). No use, distribution, or reproduction is permitted which does not comply with these terms. Permissions for commercial use of this work beyond the scope of the License (<http://www.eurjchem.com/index.php/eurjchem/pages/view/terms>) are administered by Atlanta Publishing House LLC (European Journal of Chemistry).